

# Chapter 35

## Experimental Analysis of Dynamic Deformation and Damage in Composite Sandwich Structures Subjected to Underwater Impulsive Loads

Siddharth Avachat and Min Zhou

**Abstract** The analysis of dynamic response of sandwich structures is complicated due to material heterogeneity, complex loading conditions and competing failure mechanisms. This investigation focuses on overall structural response, deformation, damage, and energy-absorption in air-backed and water-backed/submerged composite sandwich structures. The damage and failure characteristics of individual components of the sandwich structures are studied using laser-based in-situ diagnostics and postmortem analysis. Simply-supported composite sandwich plates with varying core-densities are subjected to a range of underwater impulsive loads using a novel projectile-impact based impulsive loading facility called the Underwater Shock Loading Simulator (USLS). In-situ high-speed digital imaging and postmortem analysis are used to study the dynamic deformation and failure characteristics of individual components; focusing on the effects of loading rate, core-characteristics and material heterogeneity on structural response. In finite-element simulations, the underwater blast loading intensity is considered using the Mie-Gruneisen equation-of-state of a linear Hugoniot form and core crushing is accounted for through a modified Drucker-Prager model. Results indicate that the core-density has a significant influence on dynamic deformations and failure modes. On a per-weight basis, low-density foam cores consistently outperform high-density foam cores, undergoing lesser deflections and transmitting smaller impulses. Polymeric foams experience considerable rate-effects and exhibit extensive shear cracking and collapse under high-magnitude multi-axial underwater impulsive loads. Calculations reveal a significant difference between the response of air-backed and water-backed/submerged structures. The experiments and computations offer approaches for improving the blast mitigation capabilities of submerged composite sandwich structures in the critical parts of a ship structure like keel, turbine-blades and rudders.

**Keywords** Composite materials • Blast resistance • Fluid structure interactions • Material-structure-property • Relations • Experimental mechanics

### 35.1 Introduction

Marine structures are designed to operate in hostile environments consisting of corrosive sea-water, hot and cold temperature extremes, transient dynamic loads like hull-slamming and complex three-dimensional hydrodynamic loads. Additionally, naval structures are required to withstand weapons impacts and blast loads resulting from surface and underwater explosions. Recent assessments of marine structures have demonstrated that sandwich composites can provide good blast mitigation due to their high strength-to-weight ratios and high shear-and-bending resistances. Characterization of the behavior of composite materials and polymeric foams under impulsive loading is a prerequisite for the analysis and design of effective, blast-resistant sandwich composites. Experimental and numerical studies have established that sandwich structures with thin, stiff faces and thick, low-density cores out-perform monolithic plates when deformation is dominated by bending. It has been demonstrated that overall deflection experienced by sandwich plates is significantly lesser than monolithic plates of equivalent mass [1–9]. The forces and impulses transmitted by sandwich structures are also smaller than monolithic structures [1, 4, 5]. Core design greatly influences dynamic response of sandwich structures. The dynamic strength of the core is an important factor in overall structural response. Stiff cores perform poorly while light cores exhibit higher blast mitigation.

---

S. Avachat (✉) • M. Zhou  
The George W. Woodruff School of Mechanical Engineering, Georgia Institute of Technology, Atlanta, GA 30332, USA  
e-mail: [sidavachat@gatech.edu](mailto:sidavachat@gatech.edu)

Recent assessments of blast-loaded structures show that FSI effects need can be exploited to improve blast mitigation in marine structures [5, 10–13]. Experiments focusing on different core topologies and specimen sizes have been carried out by Espinosa et al. [14] and McShane et al. [15], using gas-gun based impact loading to generate underwater pressure impulses and by Dharmasena et al. [16] using explosive sheets to generate planar pressure impulses. Shukla and co-workers [17–21] examined the dynamic response of woven E-glass composite facesheets and stitched core sandwich structures to air-based shock loading concluding that stitched cores exhibit superior mechanical performance. They also showed that sandwich structures with graded cores provide good blast mitigation.

One of the most important factors influencing the behavior of sandwich composites under dynamic loads is the dynamic strength of the core. In this paper, we report the dynamic response of sandwich composites with different core densities but identical total masses subjected to high-intensity underwater impulsive loads. The focus is on the deformations and failure modes of sandwich composites under impulsive loads, with the aim to design more blast-resistant structures. Sandwich composites are subjected to a range of underwater impulsive loads and panel responses are compared to those of monolithic fiberglass plates of equivalent mass. Planar underwater impulses are generated using a novel experimental setup called the Underwater Shock Loading Simulator (USLS). A simply-supported beam configuration is chosen because the location of the failure modes in such a setting allows accurate time-resolved measurements using high-speed digital imaging. Specifically, high-speed digital imaging enables the study of overall deflection, face-wrinkling, core-face debonding, core-compression, core shear-cracking and rupture and their dependence on load intensity and core characteristics. The impulses are measured using high-dynamic range piezoelectric pressure transducers and a high-frequency data acquisition system.

## 35.2 Materials

Fiber-matrix composites are composed of two distinct phases: (1) reinforcements like glass-fibers, carbon-fibers, and (2) matrix materials like epoxy, polyester, etc. The strength and stiffness of the finished composite is determined by the volume fraction of glass fibers and directionality of fibers with respect to external loads. The manufacturing technique used here is called Vacuum Assisted Resin Transfer Molding (VARTM). Glass-reinforced composites are stacked in a pattern to create a “quasi-isotropic” layup – (0/45/–45/90)<sub>s</sub>. This process is repeated to achieve the desired thickness of 3 mm for sandwich structures faces and 6 mm for monolithic structures. Average fiber-volume is ~60%. Material properties of the composite materials are given in

The core is made of Divinycell H-100 PVC foam [22] for which stress–strain response is described by a volumetric hardening model in which the evolution of the yield surface is driven by the volumetric plastic strain. The response consists of three distinct regimes: (1) initial nearly elastic deformation, (2) plateau region in which deformation occurs at relatively constant stress; and (3) lock-up/densification stage beyond which the material becomes fully compacted as shown in Fig. 35.1. Low yield stresses and long stress-saturated plateaus indicate that these materials can absorb significant amounts of energy. High strain-rate studies on PVC foams show a weak dependence on strain-rate [23]. Sandwich structures are constructed by joining the facesheets to the PVC foam cores using epoxy adhesive. The total areal mass of the structures is kept constant to facilitate comparison of blast resistance; this leads to 30 mm thick HP60, 20 mm thick HP100 and 10 mm thick HP200 cores.

## 35.3 Experiments

### 35.3.1 Experimental Apparatus

The Underwater Shock Loading Simulator (USLS) has been developed as part of a research effort to study the dynamic response of marine structures to underwater blast loading. A gas-gun based impact loading is used to create underwater pressure impulses. A projectile is accelerated down the length of a gas-gun barrel; after exiting the barrel it strikes a flyer plate fitted in a sealed water-chamber. The stress-wave generated inside the flyer plate is transmitted through the flyer-water interface into the water-chamber. By varying the projectile velocity and mass, pressure waves of varying magnitudes can be generated in the water-chamber. By varying the flyer-plate thickness, the decay time for the pressure wave can be changed. The pressure wave generated in the water-chamber travels down the length of the chamber (~700 mm) and impinges on the target. Figure 35.2 shows a schematic of the sectional view of the experimental setup and the placement of high-speed camera and illumination. Figure 35.3 shows the photograph of the USLS with different components. Diagnostics for the USLS consist of a high-speed camera (Imacon 200D) capable of capturing 200 million frames per second and a resolution of  $1,368 \times 1,368$ . The enclosure is fitted with transparent PMMA sheets to enable in-situ high-speed digital imaging of sandwich structures subjected to impulsive loads.

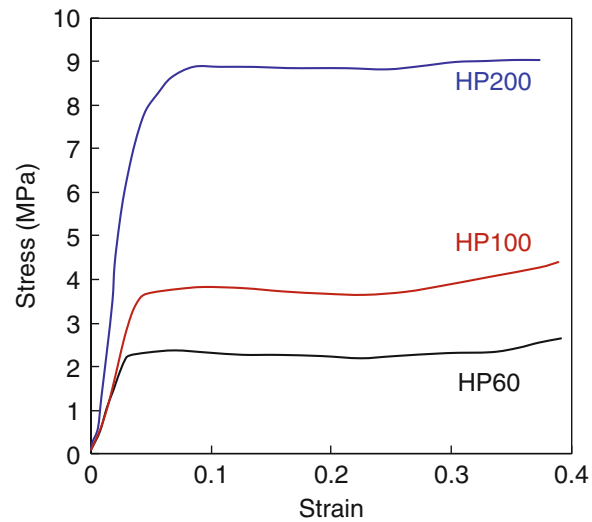


**Fig. 35.1** Stress–strain curve of HP60, HP100 and HP200 at a strain-rate of  $\sim 1,000 \text{ s}^{-1}$

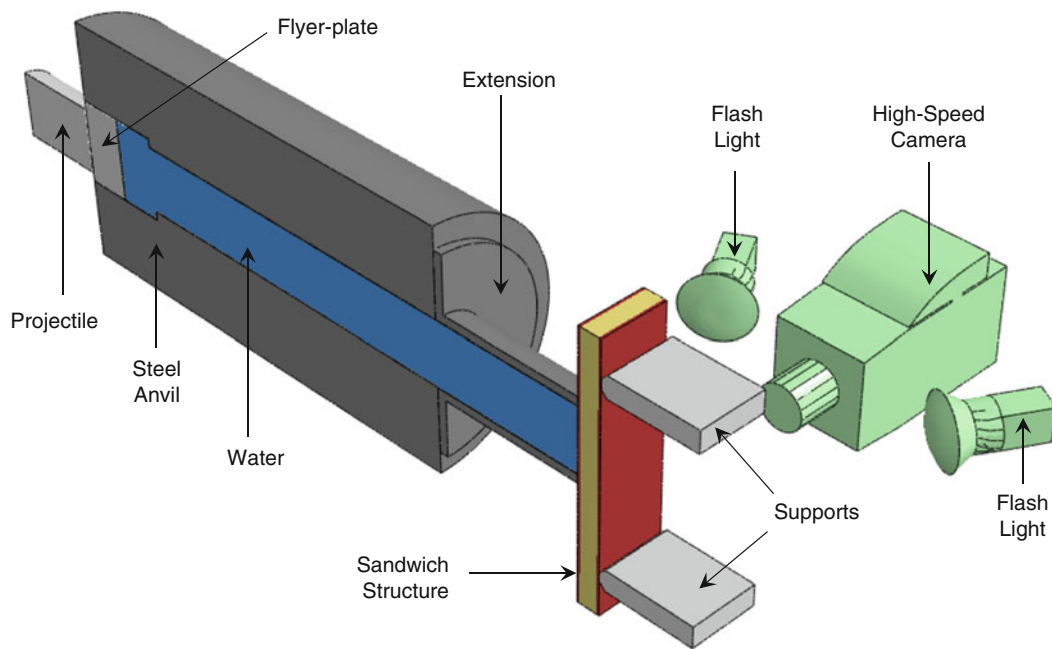


**Fig. 35.2** Sectional view of Underwater Shock Loading Simulator (USLS) and simply-supported sandwich structure showing the placement of high-speed camera and flash-lights. A high-velocity projectile hits the flyer-plate and creates a stress-wave which travels through the flyer-plate and into the water, generating an impulse identical to one produced by an underwater explosion

### 35.3.2 Loading Configurations and Impulsive Loads

Simply-supported composite sandwich structures (shown in Fig. 35.2) are subjected to underwater impulsive loads of varying magnitudes. A simply-supported loading configuration emulates the behavior of a hull with stiffeners along the side. Sandwich structures analyzed here are in the form of beam specimens of length 300 mm and width 80 mm. Simply-supported behavior and thickness to length ratio of less than 0.1 ensures beam bending behavior. The facesheet thickness is 3 mm and the core-thicknesses are adjusted to keep total mass constant. Projectiles and flyer-plates are machined from

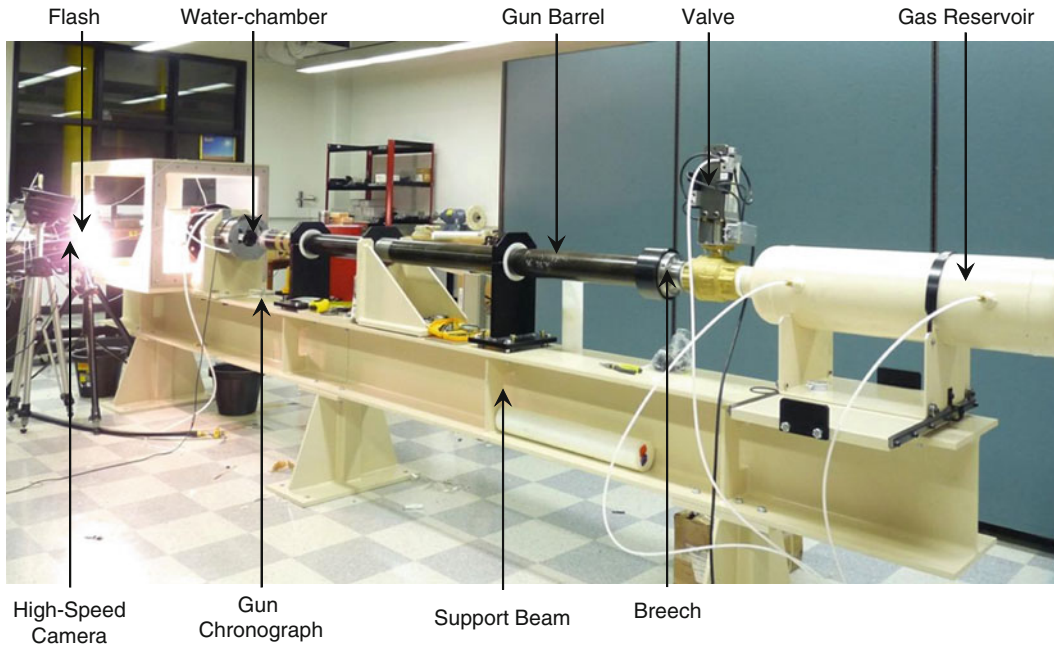


**Fig. 35.3** Photograph of the Underwater Shock Loading Simulator (USLS). Pictured are the gas-reservoir, gun-barrel, water-chamber and the Imacon 200D high-speed camera



**Fig. 35.4** Schematic of the plate-impact and transmission-reflection problem at two interfaces – (1) projectile-flyer plate and (2) flyer-plate-water

aluminum alloy and are of length 80 and 50 mm respectively. Projectiles weigh approximately 0.8 kg. When the projectile, propelled by the gas escaping from the gun-barrel, strikes the flyer-plate, it creates a compressive stress-pulse which is transmitted into the water-chamber as shown in Fig. 35.4.

The stress-wave  $\sigma(x, t)$  created when the projectile strikes the flyer-plate can be given by the equation

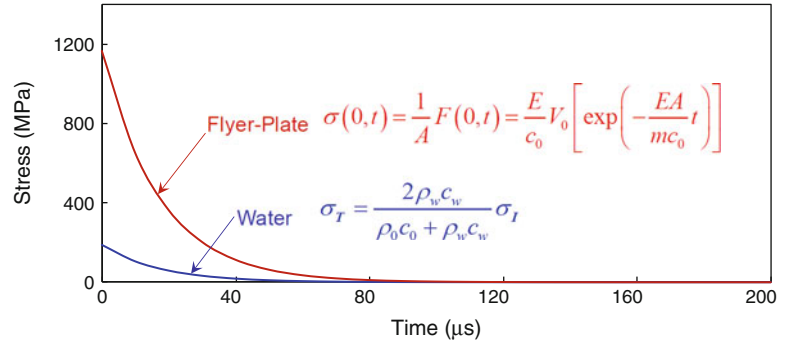
$$\sigma(0, t) = \frac{1}{A} F(0, t) = \frac{E}{c_0} V_0 \left[ \exp\left(-\frac{EA}{mc_0} t\right) \right], \quad (35.1)$$

where  $E$  is the elastic modulus of material,  $c_0$  is the speed of sound in the material,  $m$  is the mass of the projectile,  $V_0$  is the velocity of the projectile,  $A$  is the cross-sectional area of the projectile and flyer-plate and  $t$  is the time. The wave transmitted into the water-chamber  $\sigma_T$  is given by

$$\sigma_T = \frac{2\rho_w c_w}{\rho_0 c_0 + \rho_w c_w} \sigma_I, \quad (35.2)$$

where  $\sigma_I = \sigma(x, t)$ ,  $\rho_0$  is the density of flyer-plate,  $c_0$  is the speed of sound in the flyer-plate material,  $\rho_w$  is the density of water and  $c_w$  is the speed of sound in water. Figure 35.5 shows the stress-pulse due to projectile impact and the impulse transmitted in to the water-chamber. Decay time is on the order of  $\sim 200 \mu\text{s}$ .

**Fig. 35.5** The stress-wave generated when the projectile strikes the flyer-plate and the pressure-wave transmitted into the water-chamber



In the USLS, depending on the projectile velocity and mass, peak-pressures ranging from 10 to 300 MPa can be generated in the shock tube. The pressure at any point in the water-chamber is given by the equation

$$p(t) = p_0 \exp\left(-\frac{t}{t_0}\right), \quad (35.3)$$

where  $p_0$  is the peak pressure,  $t$  is time at which measurement is carried out and  $t_0$  is the decay time. The area under the curve of the pressure vs. time plot is the impulse imparted by the wave, measured in  $\text{Pa} \cdot \text{s}$ . Impulse  $I$  is given by

$$I = \int_0^t p(t) dt. \quad (35.4)$$

The non-dimensional impulse  $\bar{I}$  is given by

$$\bar{I} = \frac{I}{\rho_w c_w \sqrt{A}}, \quad (35.5)$$

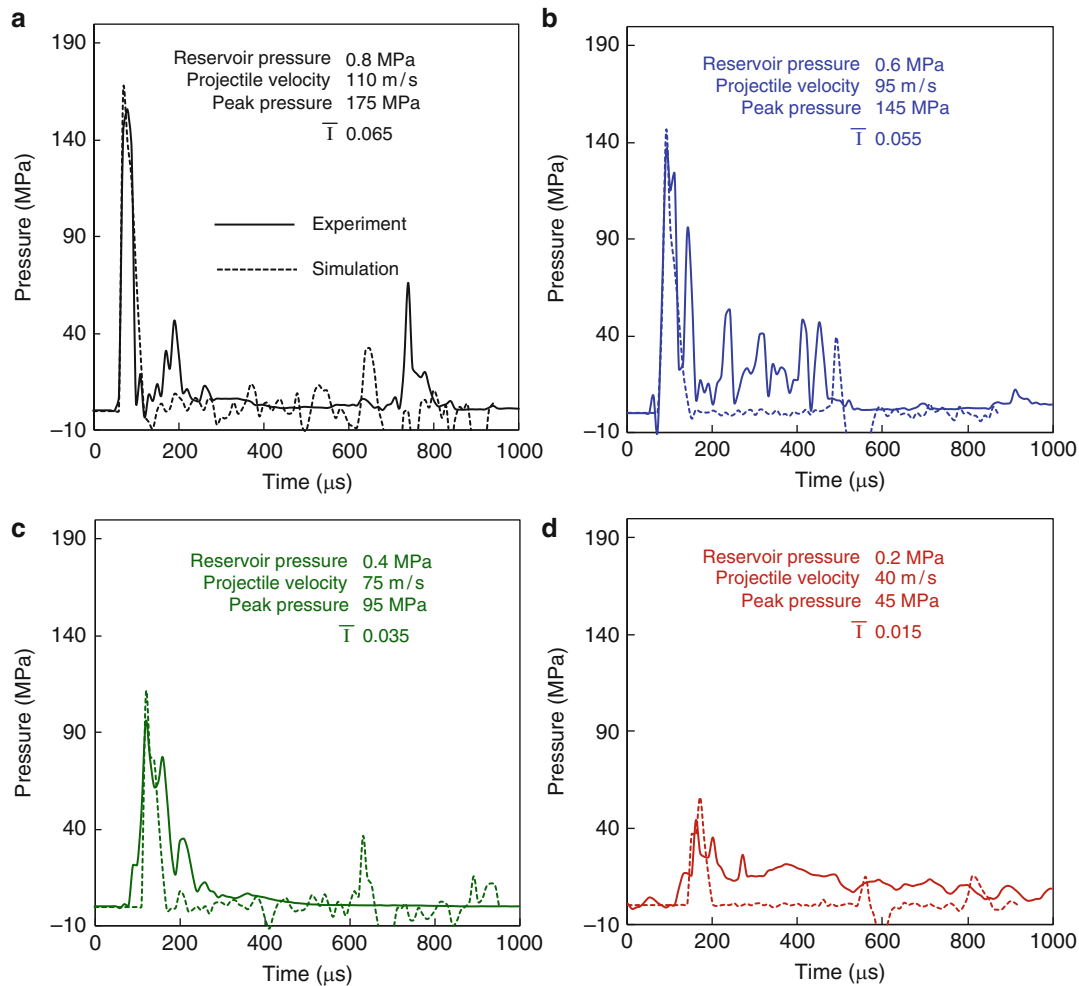
where  $I$  is impulse, calculated as the area under the curve of the pressure versus time plot,  $\rho_w$  is the density of water,  $c_w$  is the speed of sound water and  $A$  is the area under impulsive loading.

Figure 35.6 shows the pressure histories corresponding to four different projectile velocities. Pressures are measured using dynamic pressure transducers capable of maximum pressure measurement up to 500 MPa. The rise time of the pressure-pulses is on the order of 25  $\mu\text{s}$  and the decay time is on the order of 800  $\mu\text{s}$ . The solid lines show experimentally measured pressure histories while the dotted lines show the numerically calculated pressure histories. The cylindrical shape of the shock tube allows a uniform pressure to be applied to the target over the area of contact. The impulse magnitudes are  $\bar{I} = 0.015, 0.035, 0.055$  and  $0.065$ .

## 35.4 Results

The USLS provides a unique means to generate high-intensity underwater impulsive loads under well-controlled conditions. Average strain rates achieved by the USLS are  $10^4 \text{ s}^{-1}$ . Dynamic deformations and failure modes are captured by in-situ high-speed digital imaging, with the aim to characterize the fundamental mechanisms of damage and failure. Attention is focused on the earliest stages of deformation because load-carrying capacity is highest at the earliest stages.

Figure 35.7 shows a sequence of high-speed photographs for a monolithic composite plate subjected to underwater impulsive loading. The projectile velocity is 75 m/s and the peak-pressure is 95 MPa – the impulse corresponds to  $\bar{I} = 0.035$  shown in Fig. 35.6c. A thin film used for sealing the water-chamber can be seen in addition to the water coming out of the water-chamber. The deformation can be divided into two regimes – (1) flexural wave propagation and (2) overall deflection. Typically, flexural waves originate at the fluid–structure interface and travel towards the supports within  $\sim 50 \mu\text{s}$ . Overall structural deflection initiates when the back-face (in this case the entire structure) starts moving. The displacement of the back-face is tracked at the mid-plane and compared with that of other structures.

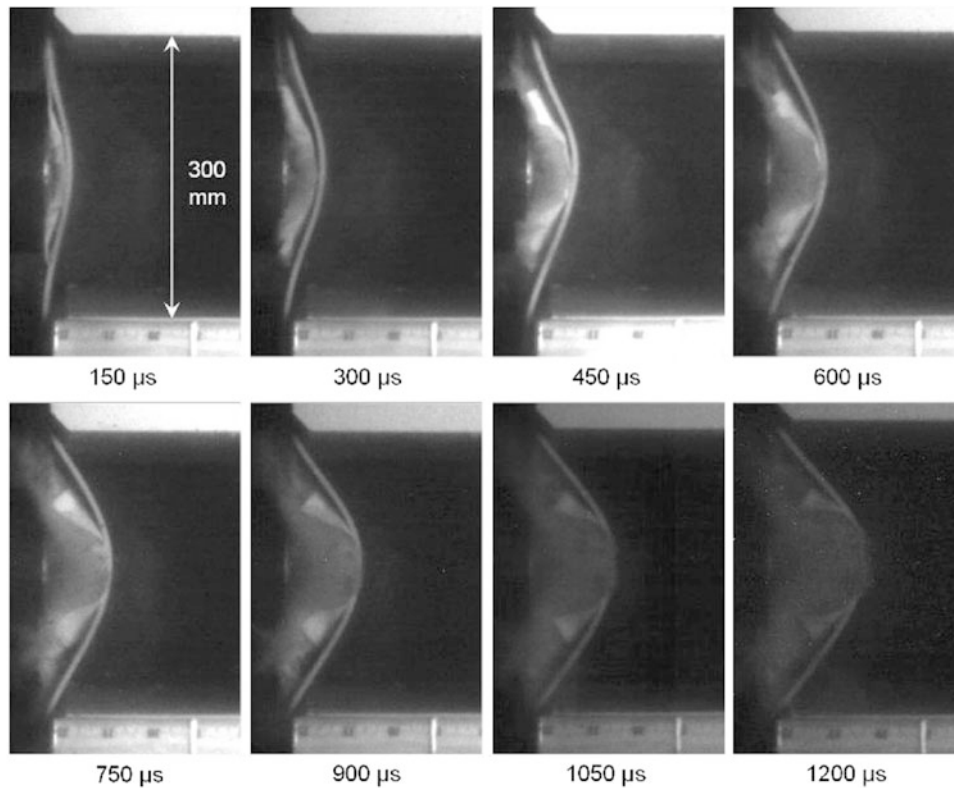


**Fig. 35.6** Comparison of numerical and experimental pressure histories in the water-chamber for four different projectile velocities and impulse magnitudes  $\bar{I} = 0.015, 0.035, 0.055$  and  $0.065$

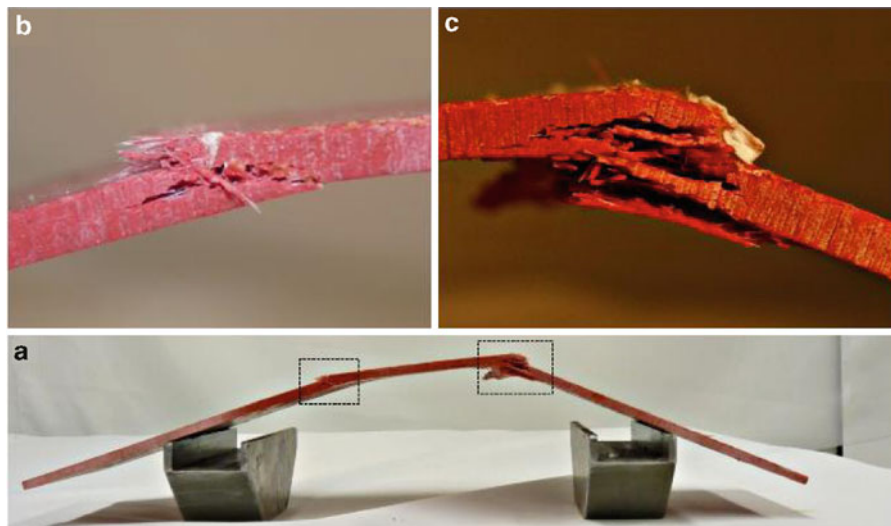
While the deformation and damage in sandwich structures can be tracked using high-speed digital imaging, the monolithic composite plate is quite thin and damage mechanisms are hard to discern. These damage mechanisms are revealed in post-mortem photographs of the monolithic composite plate – shown in Fig. 35.8a–c. Figure 35.8a shows the deformed monolithic plate with easily identifiable “hinges” formed near the loading area; Fig. 35.8b, c show delamination between successive layers in the laminate, matrix-cracking, fiber-pullout and rupture. While the deflection is relatively uniform over the length of the composite plate, damage mechanisms are predominantly observed near the circumference of the shock-tube and near the supports. This indicates a significant role of shear stresses in damage creation.

Figure 35.9 shows a sequence of high-speed photographs of a composite sandwich structure with a Divinycell HP200 core subjected to underwater impulsive loading. Immediately after the onset of deformation, flexural waves travel through the front-face, severing the core-facesheet bond. If the core-facesheet bond is very strong, a layer of core material is torn away by the facesheet due to the low tensile strength of PVC core material. Core-face debonding and core-failure, due to cracking and fragmentation, is observed at  $t = 50 \mu\text{s}$ . Core-crushing, a mechanical property that makes composite sandwich structures very attractive for marine applications commences at  $t = 150 \mu\text{s}$  and is restricted to the region close to the loading area. The back-face ruptures at  $t = 900 \mu\text{s}$ .

Figure 35.10 shows a sequence of high-speed photographs of a composite sandwich structure with a Divinycell HP100 core subjected to underwater impulsive loading. Core-facesheet debonding and composite face wrinkling failure and core-indentation can be seen at  $t = 150 \mu\text{s}$ . In this type of failure mechanism, the core-material fails in a highly localized region and causes compressive loading and buckling in the front-face. Shear-dominated cracks originate near the supports at  $t = 300 \mu\text{s}$  and lead to core fracture. Back-face ruptures at  $t = 900 \mu\text{s}$ .



**Fig. 35.7** Sequence of high-speed photographs showing the deformation in a monolithic composite plate subjected to underwater impulsive loading with  $\bar{I} = 0.035$



**Fig. 35.8** Post-mortem photographs of impulsively loaded composite plates with cross-sections showing inter-laminar delamination, matrix-cracking, fiber-matrix debonding, fiber-pullout and intra-laminar cracking

Figure 35.11 shows a sequence of high-speed photographs of a composite sandwich structure with a Divinycell HP60 core subjected to underwater impulsive loading. The dynamic response of the sandwich structure with a HP60 core is quite different than those with HP100 or HP200 cores – in that there is no core-shear cracking, front-face-wrinkling and core-face debonding. Core-compression commences immediately after the onset of loading at  $t = 150 \mu\text{s}$  and inclined cracks originate near the loading circumference area. These cracks propagate from the front-face to the back-face and branch into three

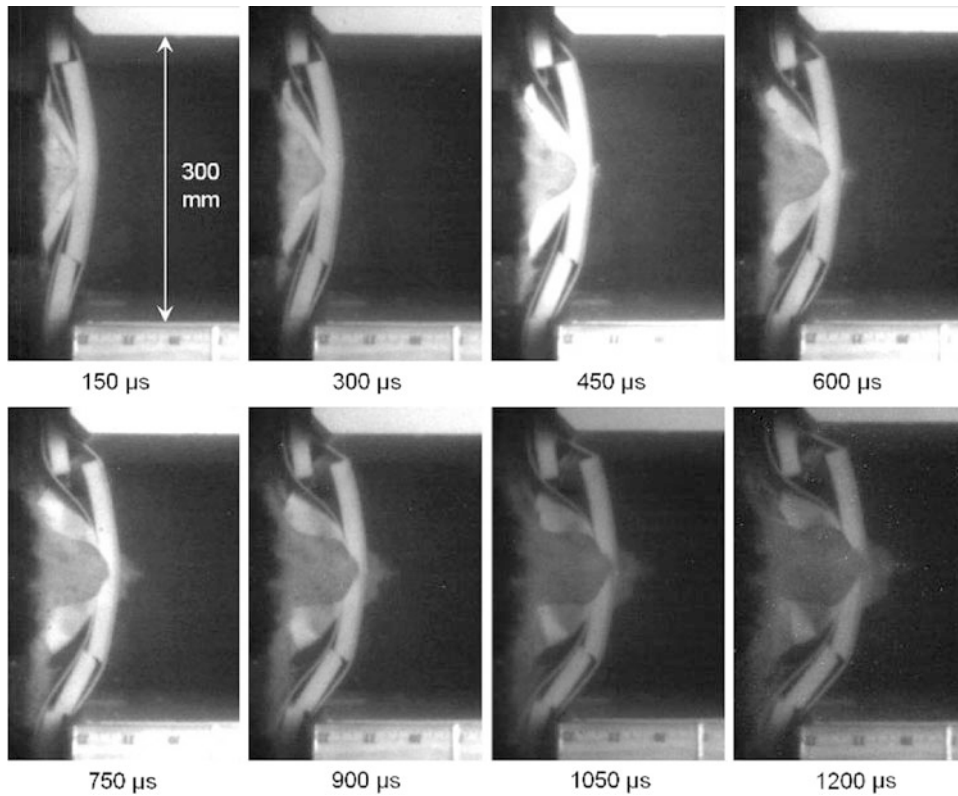


**Fig. 35.9** Sequence of high-speed photographs showing the deformation in a sandwich structure with HP200 core subjected to underwater impulsive loading with  $\bar{I} = 0.035$ . Large-scale core-front-face debonding and core-fragmentation can be observed. The core fractures prior to core-compression and rupture occurs at  $t = 900 \mu\text{s}$

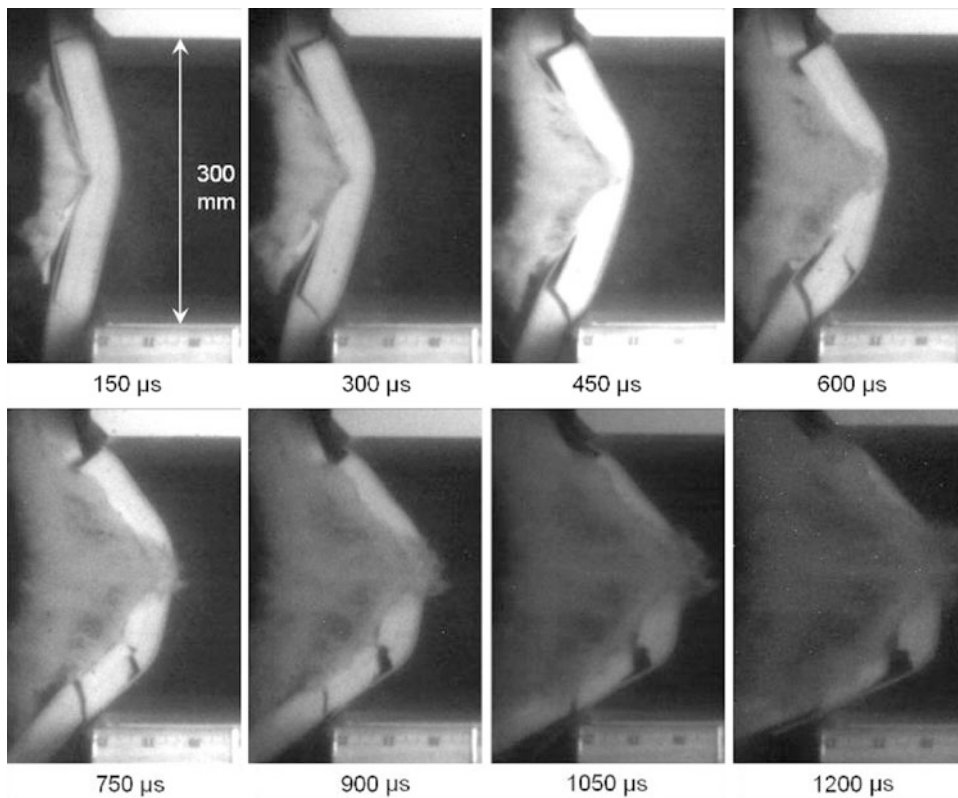


**Fig. 35.10** Sequence of high-speed photographs showing the deformation in a sandwich composite with HP100 core subjected to underwater impulsive loading with  $\bar{I} = 0.035$ . Front-face wrinkling and core-indentation occurs at  $t = 300 \mu\text{s}$ . Inclined cracks initiated at  $t = 600 \mu\text{s}$  followed by rupture at  $t = 900 \mu\text{s}$

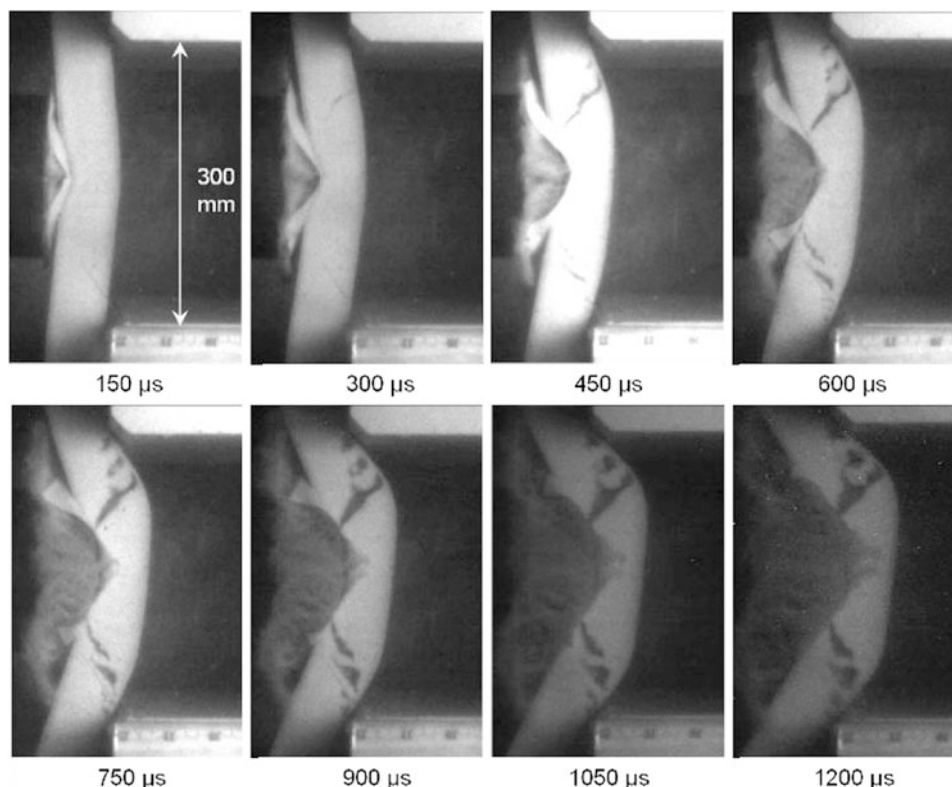


**Fig. 35.11** Sequence of high-speed photographs showing the deformation in a sandwich composite with HP60 core subjected to underwater impulsive loading with  $\bar{I} = 0.035$ . Deformation in the core is quite uniform and bending deformation occurs prior to core-cracking. Core-face debonding is relatively less widespread and facesheet wrinkling does not occur. Core-crushing occurs simultaneously with core-tensile cracking. Rupture is not observed

cracks ( at  $t = 450 \mu\text{s}$ ) near the back-face – causing core-back-face debonding. Core-compression and core-cracking occur simultaneously with crack propagation through the core. This structure does *not* experience large-scale core-face debonding or rupture of the back-face.

Comparison of the high-speed photographs of different sandwich structures subjected to identical impulsive loads reveals that core-density plays an important role in dynamic response. High-density cores undergo fracture and fragmentation prior to core-compression. These cores also experience rupture due to failure in the front and back faces. For high-density cores, failure in the front face is primarily in the form of face-wrinkling and matrix-cracking. Compared to high-density cores, low-density cores exhibit considerably different dynamic deformations. For these structures, the front-face is less susceptible to wrinkling and rupture. Core-compression occurs simultaneously with core-cracking; core-cracking is primarily due to tensile loads as a result of bending-deformation.

The time-histories of midpoint deflections for each composite structure (obtained using high-speed photographs of the side-view) are shown in Fig. 35.12. The monolithic composite structure is used as a benchmark for comparison with other structures. The lesser the deflection is compared to the monolithic composite plate; the better is the blast-resistance. Figure 35.12a shows the normalized deflection,  $\Delta/L$  (where  $\Delta$  is deflection and  $L$  is the span of the sandwich beam), of composite structures to an underwater impulsive load corresponding to  $\bar{I} = 0.035$  shown in Fig. 35.6c. Monolithic composite experiences the greatest deflection at the highest rate in comparison to the sandwich structures. The sandwich structure with HP100 core initially exhibits a rate of deformation that is identical to the sandwich structure with HP200 core but the dynamic response of HP100 core diverges at  $t = 400 \mu\text{s}$  and the rate of deflection reduces. For the sandwich structure with HP60 core, the rate of deflection is the lowest of all three sandwich structures. In terms of overall deflection at  $t = 1000 \mu\text{s}$ , the sandwich structure with HP200 core deflects  $\sim 20\%$  less than the monolithic composite, sandwich structure with HP100 core deflects  $\sim 60\%$  less than the monolithic composite and the sandwich structure with HP60 core deflects  $\sim 70\%$  less than the monolithic composite. Figure 35.12b shows the time histories of midpoint displacements of composite structures subjected to an underwater impulsive load corresponding to  $\bar{I} = 0.065$  shown in Fig. 35.6a. The deflections follow a similar trend as described for Fig. 35.12a. Due the higher load intensity, the sandwich structure with HP200 core deflects

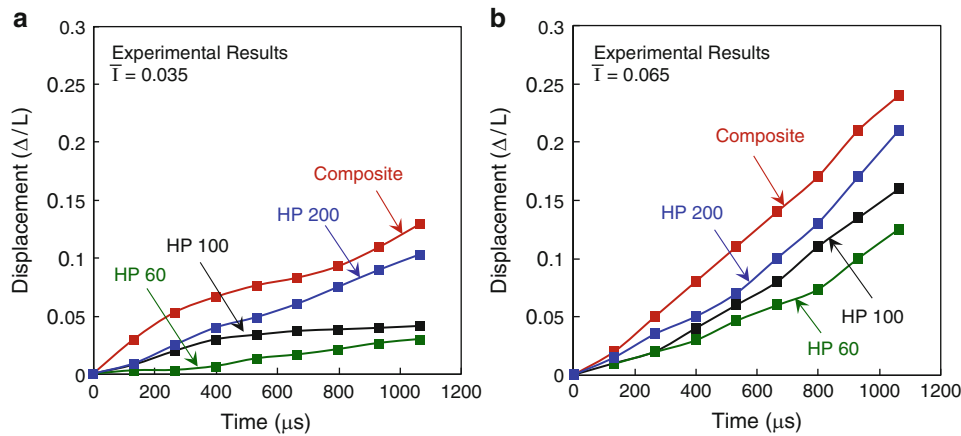


**Fig. 35.12** Experimentally measured mid-point displacements as a function of time for different structural configurations for (a)  $\bar{I} = 0.035$  and (b)  $\bar{I} = 0.065$

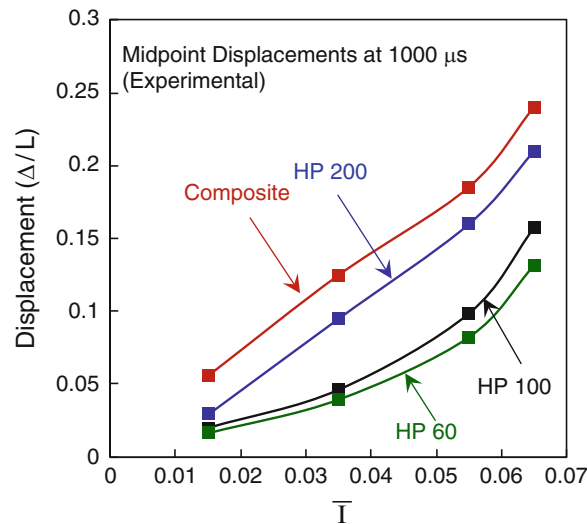


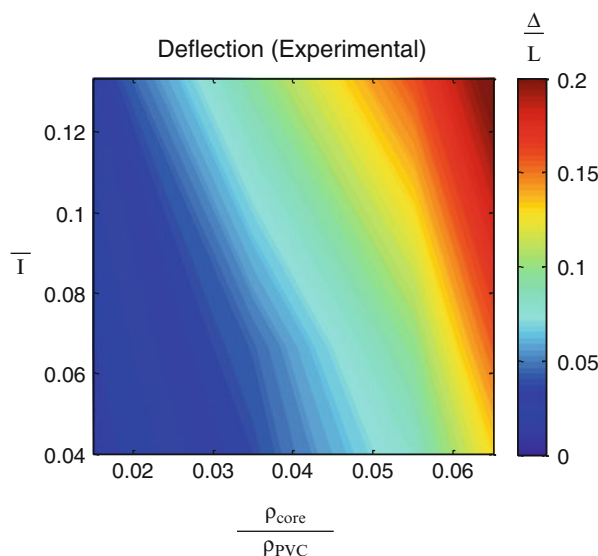
**Fig. 35.13** Displacement as a function of peak pressure for composite structures with different cores. On a per-weight basis, low-density cores consistently outperform high-density cores. Sandwich structures are superior to monolithic composite plates

$\sim 10\%$  less than the monolithic composite, sandwich structure with HP100 core deflects  $\sim 30\%$  less than the monolithic composite and the sandwich structure with HP60 core deflects  $\sim 45\%$  less than the monolithic composite.

Figure 35.13 shows the normalized deflection,  $\Delta/L$  (where  $\Delta$  is deflection and  $L$  is the span of the sandwich beam) at  $t = 1000 \mu s$  as a function of peak pressure for all the composite structures tested here. The monolithic composite shows highest deflection for all load intensities followed by the sandwich structure with HP200 core. Compared to the monolithic sandwich structure (if the  $\Delta/L$  for monolithic composite is 100%), the deflection in the sandwich structure with HP200 core is  $\sim 20\%$  smaller, that with HP100 core is  $\sim 60\%$  smaller and that with HP60 core is  $\sim 66\%$  smaller. The deflections experienced by sandwich structures with HP60 and HP100 cores are comparable, with the HP60 core outperforming the HP100 core by a slender margin – particularly at higher load intensities.

To obtain material-property-performance relationships, dimensional analysis is carried out. The impulse is normalized using equation (5), the core-properties are normalized by dividing the core-density by the density of the parent material (in this case PVC). The measured quantities – deflection and force are plotted as functions of normalized impulse,  $\bar{I}$ , and normalized density,  $\rho_{core}/\rho_{PVC}$ , in Fig. 35.14a, b respectively. The contour plots demonstrate that at low values of  $\bar{I}$ , deflection and reaction-force are both relatively insensitive to  $\rho_{core}/\rho_{PVC}$ . However, as  $\bar{I}$  increases, high-density cores i.e. higher values of  $\rho_{core}/\rho_{PVC}$  show a reduction in blast resistance. In terms of deflection and reaction-force, the performance of

**Fig. 35.14** Material-property-performance map showing deflection ( $\Delta/L$ ) as a function of material properties ( $\rho_{core}/\rho_{PVC}$ ) and the load intensity ( $\bar{I}$ ). The contours show that low-density cores undergo lesser deflection and consistently outperform high-density cores on a per-weight basis



HP60 and HP100 is closer, but HP60 slightly outperforms HP100 cores. Clearly, provided the dimensional requirements are satisfied, thick cores of low-density foams consistently provide the highest blast-mitigation to underwater impulsive loads.

### 35.5 Conclusions

An experimental characterization of the dynamic response of sandwich composites subjected to high-intensity underwater impulsive loads is presented. A new gas-gun based experimental facility is used to generate a range of impulsive loads. The deformation and failure modes in sandwich structures are studied using high-speed digital imaging. Experiments show that the core plays an important role in the dynamic response of sandwich composites. The density and stiffness of the core determines the failure mode experienced by the sandwich structure. Monolithic composites subjected to impulsive loads undergo matrix-cracking, delamination and fiber-pullout and form characteristic hinges near the loading circumference. HP200 cores undergo face-wrinkling, large-scale shear cracking and fragmentation, followed by core-crushing and ultimately rupture. HP100 cores experience core-indentation failure due in which the core experiences collapses in a small region and the front-face ruptures. This is followed by cracking and overall bending response. HP60 cores exhibit simultaneous core-compression and tensile cracking. Face-wrinkling is negligible and rupture is not observed.

Time-resolved deflections measured by high-speed photography indicate that sandwich structures are superior to monolithic structures. Low-density cores consistently outperform high-density cores, undergoing lesser deflections at all impulse magnitudes. For high magnitude impulsive loads, the sandwich structure with HP200 core deflects  $\sim 10\%$  less than the monolithic composite, sandwich structure with HP100 core deflects  $\sim 30\%$  less than the monolithic composite and the sandwich structure with HP60 core deflects  $\sim 45\%$  less than the monolithic composite.

Uniaxial testing has shown that the dynamic response of polymeric foam cores exhibit mild strain-rate dependence. However, under complex multi-axial loads, the strain-rate effects are significantly higher. Strain-rate effects are much more pronounced for HP200 cores and are less dominant for HP100 and HP60 cores. The differing trends in structural response reflect the effects of different deformation and failure mechanisms in foams and fiber-reinforced composites under impulsive loads. The USLS provides a useful means with which the comparative load-carrying capacity in sandwich composites under dynamic loads can be obtained experimentally. The underlying trends in dynamic response are revealed by design maps which incorporate material properties, impulse magnitudes and deflections.

## References

1. Liang YM et al (2007) The response of metallic sandwich panels to water blast. *J Appl Mech Trans ASME* 74(1):81–99
2. Dharmasena KP et al (2010) Dynamic compression of metallic sandwich structures during planar impulsive loading in water. *European J Mech Solids* 29(1):56–67
3. Wei Z et al (2008) The resistance of metallic plates to localized impulse. *J Mech Phys Solids* 56(5):2074–2091
4. Xue ZY, Hutchinson JW (2003) Preliminary assessment of sandwich plates subject to blast loads. *Int J Mech Sci* 45(4):687–705
5. Xue ZY, Hutchinson JW (2004) A comparative study of impulse-resistant metal sandwich plates. *Int J Impact Eng* 30(10):1283–1305
6. Hutchinson JW, Xue ZY (2005) Metal sandwich plates optimized for pressure impulses. *Int J Mech Sci* 47(4–5):545–569
7. Qiu X, Deshpande VS, Fleck NA (2003) Finite element analysis of the dynamic response of clamped sandwich beams subject to shock loading. *European J Mech Solids* 22(6):801–814
8. Fleck NA, Deshpande VS (2004) The resistance of clamped sandwich beams to shock loading. *J Appl Mech Trans ASME* 71(3):386–401
9. Qiu X, Deshpande VS, Fleck NA (2004) Dynamic response of a clamped circular sandwich plate subject to shock loading. *J Appl Mech Trans ASME* 71(5):637–645
10. Hutchinson JW (2009) Energy and momentum transfer in air shocks. *J Appl Mech Trans ASME* 76(5):1–7
11. Kambouchev N, Radovitzky R, Noels L (2007) Fluid–structure interaction effects in the dynamic response of free-standing plates to uniform shock loading. *J Appl Mech Trans ASME* 74(5):1042–1045
12. Deshpande VS, Fleck NA (2005) One-dimensional response of sandwich plates to underwater shock loading. *J Mech Phys Solids* 53(11):2347–2383
13. Vaziri A, Hutchinson JW (2007) Metal sandwich plates subject to intense air shocks. *Int J Solids Struct* 44(6):2021–2035
14. Espinosa HD, Lee S, Moldovan N (2006) A novel fluid structure interaction experiment to investigate deformation of structural elements subjected to impulsive loading. *Exp Mech* 46(6):805–824
15. McShane GJ et al (2008) Dynamic rupture of polymer-metal bilayer plates. *Int J Solids Struct* 45(16):4407–4426
16. Dharmasena KP et al (2008) Mechanical response of metallic honeycomb sandwich panel structures to high-intensity dynamic loading. *Int J Impact Eng* 35(9):1063–1074
17. Tekalur SA, Bogdanovich AE, Shukla A (2009) Shock loading response of sandwich panels with 3-D woven E-glass composite skins and stitched foam core. *Compos Sci Technol* 69(6):736–753
18. Tekalur SA, Shukla A, Shivakumar K (2008) Blast resistance of polyurea based layered composite materials. *Compos Struct* 84(3):271–281
19. LeBlanc J et al (2007) Shock loading of three-dimensional woven composite materials. *Compos Struct* 79(3):344–355
20. Grogan J et al (2007) Ballistic resistance of 2D and 3D woven sandwich composites. *J Sandwich Struct Mater* 9(3):283–302
21. Wang EH, Gardner N, Shukla A (2009) The blast resistance of sandwich composites with stepwise graded cores. *Int J Solids Struct* 46(18–19):3492–3502
22. DIAB Inc., S.D., DeSoto, Texas 75115, USA. [http://www.diabgroup.com/europe/literature/e\\_pdf\\_files/man\\_pdf/H\\_man.pdf](http://www.diabgroup.com/europe/literature/e_pdf_files/man_pdf/H_man.pdf). Accessed 5 May 2011
23. Tagarielli VL, Deshpande VS, Fleck NA (2008) The high strain rate response of PVC foams and end-grain balsa wood. *Compos Part B Eng* 39(1):83–91